A Novel Electromagnetic Radiation Source Localization Method Based on Dynamic Data Driven Simulations

Xu Xie(✉) and Yuqing Ma

College of Systems Engineering, National University of Defense Technology, Changsha, China
x.xie@hotmail.com

Abstract. Locating enemy targets via their electromagnetic radiation signal is vital to block and attack the enemy targets at an earlier stage. Traditional electromagnetic radiation source localization methods in literature are essentially geometric methods. Although they are simple and intuitive, they might fail to locate the source due to measurement noise. This paper proposes a novel electromagnetic radiation source localization method based on dynamic data driven simulations. In the proposed approach, we first model the spatial propagation process of the electromagnetic radiation signal emitted from the target, and then we assume a proper model for the noisy measurements. Based on the signal propagation model and the measurement model, the particle filter is employed to estimate the target position, and in the process addresses measurement and modeling errors. Identical-twin experiment is conducted to test and validate the proposed approach. The simulation results show that the proposed method can accurately locate the electromagnetic radiation source, and is robust to errors both in the model and in the data.

Keywords: Electromagnetic radiation source localization · Signal propagation modeling · Dynamic data driven simulation · Particle filters

1 Introduction

At the end of the 19th century, the discovery of wireless electromagnetic waves not only provided a new information carrier for communication, but also could be used to locate and trace the source of electromagnetic radiation. In the military field, especially the ocean security, the main threats are to prevent the invasion of enemy fleets, prevent drone reconnaissance, and prevent submarines from sneaking in, etc. If we could locate the targets by detecting their electromagnetic radiation signals, we would be able to block and attack the enemy targets at an earlier stage.

In literature, the commonly used electromagnetic radiation source localization methods can be classified into four categories, namely the Received Signal

W. Fan et al. (Eds.): AsiaSim 2022, CCIS 1713, pp. 348–359, 2022.
https://doi.org/10.1007/978-981-19-9195-0_28

Strength (RSS) method, the Time of Arrival (TOA) method, the Time Difference of Arrival (TDOA) method, and the Angle of Arrival (AOA) method [1]. The RSS method is designed based on the fact that the power of the wireless signal will decay according to a certain law as the signal propagates spatially [2]. The RSS method first records the signal power received at each measurement point, and then calculates the distances between the measurement points to the target based on a semi-empirical model, and finally exploits the triangulation theory to estimate the location of the target. The TOA method is proposed based on the principle that the product of the speed and time is equal to the travel distance [3]. The target sends electromagnetic wave signal, and each measurement point receives and records the arrival time of the signal; based on the transmission media, the travel speed can be determined, and then the travel distance can be calculated accordingly. Finally, the triangulation theory is again used to locate the target. When using the TOA method, it is necessary to ensure that the clocks among all measurement points are strictly synchronized, otherwise the localization error would be large. Due to this limitation, [4] proposes the TDOA method, which locates the target according to the difference among time instants when signal arrives at each measurement points, thereby reducing the time synchronization requirements. The AOA method uses a receiver to measure the angle of the signal emitted from the target to each measurement point, and uses geometric relations to estimate the coordinates of the target. The advantage of the AOA method is that it does not require time synchronization, but it is susceptible to be affected by wave reflection.

The electromagnetic radiation source localization methods in literature are essentially geometric methods, and their advantages are that they are simple and intuitive, but in practical applications, measurement noise inevitably exist, which will result in failures when using these methods, since the intersection point (i.e. the estimated target position) may not exist or multiple intersection points exist. Therefore, this paper proposes a novel electromagnetic radiation source localization method based on dynamic data driven simulations (DDDS). Dynamic data driven simulations are a new simulation paradigm, where the simulation is continually influenced by the real time data for better analysis and prediction of a system under study [5,6]. In a dynamic data driven simulation, the noisy observations from the system under study are continually injected into the simulation which mimics the dynamic state evolution of the system. At the meantime, the data assimilation technique [7] is exploited to combine noisy observations and (simulation) model predictions to estimate the system state. In the proposed approach, we first model the spatial propagation process of the electromagnetic radiation signal emitted from the target, and then we assume a proper model for the noisy measurements. Based on the signal propagation model and the measurement model, the particle filter [8,9] is employed to estimate the target position. Identical-twin experiment is conducted to test and validate the proposed approach. The simulation results show that the proposed method can accurately locate the electromagnetic radiation source.

The rest of the paper is organized as follows. We first overview the dynamic data driven simulations in Sect. 2. Section 3 then models the spatial propagation process of the electromagnetic radiation signal emitted from the target, after which Sect. 4 presents the electromagnetic radiation source localization method based on dynamic data driven simulations in detail. The simulation study to test the proposed approach is presented in Sect. 5, and finally, the paper is concluded in Sect. 6.

2 Dynamic Data Driven Simulation

Modeling & Simulation are a method of choice for studying and predicting dynamic behavior of complex systems. However, models inevitably contain errors, which arise from many sources in the modeling process, such as inadequate sampling of the real system when constructing the behavior database for the source system [10], or conceptual abstraction in the modeling process [11]. Due to these inevitable errors, even elaborate complex models of systems cannot model the reality perfectly, and consequently, results produced by these imperfect simulation models will diverge from or fail to predict the real behavior of those systems [12,13]. With the advancement of measurement infrastructures, such as sensors, data storage technologies, and remote data access, the availability of data, whether real-time on-line or archival, has greatly increased [12,13]. This allows for a new paradigm – *dynamic data driven simulations*, in which the simulation is continuously influenced by fresh data sampled from the real system [5].

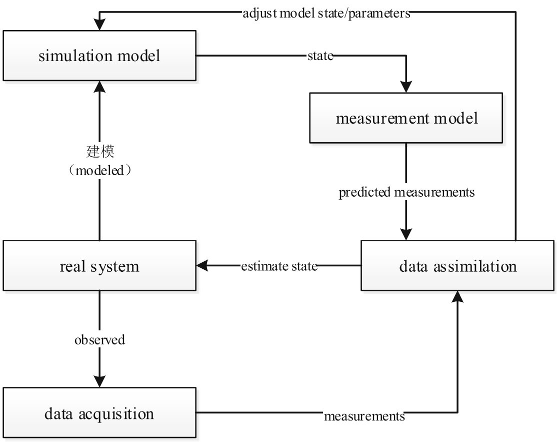

Fig. 1. A general dynamic data driven simulation [6]

Figure 1 shows a general dynamic data driven simulation, which consists of 1) a simulation model, describing the dynamic behavior of the real system; 2) a data acquisition component, which essentially consists of sensors that collect data from the real system; and 3) a data assimilation component, which carries out state estimations based on information from both measurements and the simulation [7,14]. Since the state evolution of a simulation system usually contains nonlinear and/or non-Gaussian behavior, the particle filter is always adopted to conduct data assimilation in dynamic data driven simulations. The particle filters approximate a probability density function by a set of particles and their associated importance weights, and therefore they put no assumption on the properties of the system model. As a result, they can effectively deal with nonlinear and/or non-Gaussian applications [15].

By assimilating actual data, the simulation can dynamically update its current state to be closer to the real system state, which facilitates real-time applications of simulation models, such as real-time control and analysis, real-time decision making, and understanding the current state of the real system. Besides, if the model state is extended to include model parameters, on-line model parameter calibration can be achieved together with the state estimation [16]. With more accurate model state and model parameters adjusted by assimilating real-time data, we can experiment (off-line) on the simulation model with the adjusted state and parameters, which will lead to more accurate results for follow-on simulations [6].

3 Spatial Propagation Model of Electromagnetic Radiation Signal

After the electromagnetic radiation signal is emitted from the target, it will be received by receivers after attenuating, delay and adding noise. The received signal can be described as:

$$r_i(t) = \mu_i s(t - \tau_i) e^{j2\pi f_i t} + n_i(t) \tag{1}$$

where $s(t)$ represents the signal emitted by the target at time t, and τ_i is the path propagation delay from the source to the i-th receiver; μ_i is the propagation path gain coefficient from the target to the i-th receiver; f_i is the drift value of the frequency caused by the Doppler effect; n_i is a complex noise; $r_i(t)$ is a complex number that represents the signal received by the receiver at time t.

3.1 Electromagnetic Radiation Signal $s(t)$

The electromagnetic radiation signal emitted by the target can be expressed as:

$$s(t) = |s| e^{j2\pi f t} \tag{2}$$

where f is the frequency of the signal in hertz (Hz), $|s|$ is the amplitude of the signal, and the unit is watts (W).

3.2 Propagation Path Gain Coefficient μ_i

The propagation path gain coefficient $|\mu_i|$ represents the power gain rate of the signal from the sender (i.e. the target) to the receiver. After the signal arrives at the receiver, it is filtered, and amplified by a low-noise amplifier (LNA), and finally sampled. So $|\mu_i|$ is related to the length of the propagation path and the magnification of the LNA. Due to the phase inconsistency between the sender and the receiver, there will exist an amplitude angle for μ_i. Therefore, we model the propagation path gain coefficient $|\mu_i|$ as:

$$\mu_i = |\mu_i| e^{j2\pi(f-f_r^i)} = \frac{k_i e^{j2\pi(f-f_r^i)}}{|\boldsymbol{P}_i(t) - \boldsymbol{G}|} \tag{3}$$

where f_r^i is the center frequency of the i-th receiver, and $2\pi(f - f_r^i)$ represents the phase difference between the sender and the receiver. $\boldsymbol{P}_i(t)$ is the position of the i-th receiver, while $\boldsymbol{G} = [g_x, g_y, g_z]^T$ is the position of the target. k_i is the LNA magnification in decibels (dB).

3.3 The Frequency Drift f_i

The moving receiver will cause the Doppler effect, which will incur the frequency drift. The frequency drift value of the i-th receiver can be expressed by:

$$f_i = \frac{v_i \cos(\theta_i)}{\lambda} = \frac{v_i f \cos(\theta_i)}{c} \tag{4}$$

where

$$\begin{aligned}
&\cos(\theta_i) = \frac{(\boldsymbol{G} - \boldsymbol{P}_i(t)) \cdot (\boldsymbol{P}_i(t - \Delta t) - \boldsymbol{P}_i(t))}{|\boldsymbol{G} - \boldsymbol{P}_i(t)| \times |\boldsymbol{P}_i(t - \Delta t) - \boldsymbol{P}_i(t)|} \\
&\boldsymbol{G} - \boldsymbol{P}_i(t) = [g_x - (x_0^i + v_x^i \times t), g_y - (y_0^i + v_y^i \times t), g_z - (z_0^i + v_z^i \times t)]^T \\
&\boldsymbol{P}_i(t - \Delta t) - \boldsymbol{P}_i(t) = [-v_x^i \times \Delta t, -v_y^i \times \Delta t, -v_z^i \times \Delta t]^T
\end{aligned}$$

where $[x_0^i, y_0^i, z_0^i]^T$ is the initial position of the i-th receiver, and $v_i = [v_x^i, v_y^i, v_z^i]^T$ is its velocity, and Δt is the sampling period of the signal.

3.4 The Received Signal at the i-th Receiver

Bring the electromagnetic radiation signal $s(t)$ (Eq. (2)), the propagation path gain coefficient μ_i (Eq. (3)), and the frequency drift f_i (Eq. (4)) into Eq. (1), we can get the signal received by the i-th receiver at time t:

$$\begin{aligned}
r_i(t) &= \mu_i s(t - \tau_i) e^{j2\pi f_i t} + n_i(t) \\
&= \frac{k_i |s|}{|\boldsymbol{P}_i(t) - \boldsymbol{G}|} e^{j(2\pi(f - f_r^i) + 2\pi f(t - \frac{|\boldsymbol{P}_i(t) - \boldsymbol{G}|}{c}) + 2\pi \frac{v_i f \cos(\theta_i)}{c})} + n_i(t)
\end{aligned} \tag{5}$$

where $\tau_i = \dfrac{|\boldsymbol{P}_i(t) - \boldsymbol{G}|}{c}$ is the signal transmission delay, and c is the speed of light.

4 The Electromagnetic Radiation Source Localization Approach

In this section, the proposed electromagnetic radiation source localization approach is presented. Since the proposed approach is based on the DDDS framework, we first formalize the system model which describes the moving of the target in Sect. 4.1, after which we assume the measurement model in Sect. 4.2 based on the spatial propagation model of electromagnetic radiation signal emitted by the target which is derived in Sect. 3. Finally, particle filters are employed to locate the target, which is described in Sect. 4.3.

4.1 System Model

The position of the target is $\boldsymbol{G} = [g_x, g_y, g_z]^T$, so we define the system state as $s_k = [g_x, g_y, g_z]^T$. In this paper, we assume that the target keeps still, therefore we can define the state evolution of the target as a slow-change process:

$$s_k = s_{k-1} + \nu_{k-1}, k = 1, 2, \dots \tag{6}$$

where the noise vector ν_{k-1} is a Gaussian white noise with an average of 0 and variances of $\sigma^2_{g_x}$, $\sigma^2_{g_y}$, $\sigma^2_{g_z}$, respectively.

4.2 Measurement Model

Suppose we have n receivers, and the measurement at the k-th step can be defined as $m_k = [r_1(k \times \Delta t), \cdots, r_n(k \times \Delta t)]^T$, where Δt is the signal sampling period of the receiver. According to the signal propagation model derived in Sect. 3, the measurement model can be defined as:

$$\begin{aligned} m_k &= g(s_k) + \varepsilon_k \\ &= \begin{bmatrix} \frac{k_1|s|}{|\boldsymbol{P}_1(k\times\Delta t)-\boldsymbol{G}|} e^{j(2\pi(f-f_r^1)+2\pi f(k\times\Delta t-\frac{|\boldsymbol{P}_1(k\times\Delta t)-\boldsymbol{G}|}{c})+2\pi\frac{v_1 f\cos(\theta_1)}{c})} \\ \vdots \\ \frac{k_n|s|}{|\boldsymbol{P}_n(k\times\Delta t)-\boldsymbol{G}|} e^{j(2\pi(f-f_r^n)+2\pi f(k\times\Delta t-\frac{|\boldsymbol{P}_n(k\times\Delta t)-\boldsymbol{G}|}{c})+2\pi\frac{v_n f\cos(\theta_n)}{c})} \end{bmatrix} + \varepsilon_k \end{aligned} \tag{7}$$

where $\cos(\theta_i), |\boldsymbol{P}_i(k \times \Delta t) - \boldsymbol{G}|, i = 1, \dots, n$ are defined in Sect. 3.3. ε_k is the measurement noise, and we assume that both the real and imaginary parts of ε_k are Gaussian white noise with mean 0 and variance σ^2_m.

4.3 Locating the Target Using Particle Filters

Based on the system model and the measurement model, we locate the target based on particle filters (see Algorithm 1). The input of the algorithm is the data sequence collected by n receivers, i.e. $data = \{[d_k^1, \cdots, d_k^n]^T\}_{k=1}^N$, where N is the number of time steps; particle filters estimate the target position as

$\{\{[g^i_{x,k}, g^i_{y,k}, g^i_{z,k}]^T\}_{i=1}^{N_p}\}_{k=1}^N$, where N_p is the number of particles. Note that at step k, the output of the particle filter is a group of particles $\{[g^i_{x,k}, g^i_{y,k}, g^i_{z,k}]^T\}_{i=1}^{N_p}$, approximating the probability distribution of the target position. Therefore, given the particles at each step k, the position of the target and the corresponding variance can be estimated:

$$[\hat{g}_{x,k}, \hat{g}_{y,k}, \hat{g}_{z,k}]^T = [\frac{1}{N_p}\sum_{i=1}^{N_p} g^i_{x,k}, \frac{1}{N_p}\sum_{i=1}^{N_p} g^i_{y,k}, \frac{1}{N_p}\sum_{i=1}^{N_p} g^i_{z,k}]^T$$

$$\sigma^2_{x,k} = \frac{1}{N_p - 1}\sum_{i=1}^{N_p}(g^i_{x,k} - \hat{g}_{x,k})^2$$

$$\sigma^2_{y,k} = \frac{1}{N_p - 1}\sum_{i=1}^{N_p}(g^i_{y,k} - \hat{g}_{y,k})^2$$

$$\sigma^2_{z,k} = \frac{1}{N_p - 1}\sum_{i=1}^{N_p}(g^i_{z,k} - \hat{g}_{z,k})^2$$

4.4 Weight Computation

Given the particle state s^i_k, we can calculate $m^i_k = [r^i_1(k\Delta t), \cdots, r^i_n(k\Delta t)]^T$ according to the measurement model. Then the particle weight can be computed as:

$$w^i_k = w^i_{k-1} \times p([d^1_k, \cdots, d^n_k]^T | m^i_k) = w^i_{k-1} \times \prod_{j=1}^{n} \frac{1}{\sqrt{2\pi}\sigma_m} e^{-\frac{|r^i_j(k\Delta t) - d^j_k|^2}{2\sigma^2_m}} \tag{8}$$

Note that $r^i_j(k\Delta t)$ and d^j_k are complex numbers, and $|r^i_j(k\Delta t) - d^j_k|$ represents the modulo of the difference between two complex numbers.

5 Experimental Results and Analysis

5.1 Experiment Scenario and Parameter Setting

We use the identical-twin experiment [17] to test and validate the proposed approach. In the identical-twin experiment, a simulation is first run, and the corresponding data are recorded. This simulation is regarded as the 'real' system. Then we add noise to these data, and use these noisy data to estimate the position of the target based on the proposed approach. Finally we compare the estimated results with the ground truth data to quantify the accuracy of the estimation.

In the first simulation which is used to generate the ground truth data, the parameters of the target are set based on Table 1. Four drones are used as receivers to collect data (i.e. the amplitude and phase of the signal), and the

Algorithm 1: The particle filter for electromagnetic radiation source localization

Input: $data = \{[d_k^1, \cdots, d_k^n]^T\}_{k=1}^N$

Output: estimated location of the target: $\{\{[g_{x,k}^i, g_{y,k}^i, g_{z,k}^i]^T\}_{i=1}^{N_p}\}_{k=1}^N$

% the initialization step

for $i = 1 : N_p$ **do**

  generate the i-th particle $s_0^i = [g_{x,0}^i, g_{y,0}^i, g_{z,0}^i]^T$

  set weight $w_0^i = 1/N_p$

end

for $k = 1 : N$ **do**

  % the sampling step for any time $k \geq 1$

  for $i = 1 : N_p$ **do**

    according to the state at time step $k-1$, i.e. s_{k-1}^i, generate a new particle at time step k, i.e. s_k^i, using equation (6)

    calculate m_k^i based on s_k^i using equation (7), and update the weight of the particle (see more details in section 4.4):

$$w_k^i = w_{k-1}^i \times p([d_k^1, \cdots, d_k^n]^T | m_k^i)$$

  end

  normalizes the particle weights and denote them as $\{s_k^i, w_k^i\}_{i=1}^{N_p}$

  % The resampling step

  resample $\{s_k^i, w_k^i\}_{i=1}^{N_p}$ using the standard resampling method which samples particles in proportion to their weights; the resampled results are again denoted as $\{s_k^i, w_k^i\}_{i=1}^{N_p}$

  Set the weight of each particle as $1/N_p$

  % record data for estimation

  record each particle's estimate of the target position: $\{[g_{x,k}^i, g_{y,k}^i, g_{z,k}^i]^T\}_{i=1}^{N_p}$

end

relevant parameters are set based on Table 2. The drones collect the data every second (i.e. $\Delta t = 1\ s$) for a total of 100 s (i.e. $N = 100$). For data noise, we set σ_m to 5% of the signal amplitude. For model errors, we set σ_{g_x}, σ_{g_y} and σ_{g_z} to 5% of the corresponding coordinates of the target position.

5.2 The Performance Indicators

In order to quantify the accuracy of the proposed localization method, we define the following performance indicators (since the z-coordinate of the target is 0, the localization error of the z-coordinate is not considered):

$$\begin{aligned} RMSE_x &= \sqrt{\frac{\sum_{k=1}^N (\hat{g}_{x,k} - g_x)^2}{N}} \\ RMSE_y &= \sqrt{\frac{\sum_{k=1}^N (\hat{g}_{y,k} - g_y)^2}{N}} \end{aligned} \tag{9}$$

Table 1. The parameter settings of the target

Parameter	Value
Position of the target	$(-9960.3, 123686, 0)$
Signal amplitude $\|s\|$	200 W
The frequency of the signal f	100 MHz

Table 2. The parameter settings of the drones (i.e. the receivers used in the experiment)

Parameter	Value
Initial position of drone#1	$(-120341, 110974, 12000)$
Velocity of drone#1	$(69, 72.4, 0)$
Initial position of drone#2	$(68625, 131345, 12000)$
Velocity of drone#2	$(58.5, 81.1, 0)$
Initial position of drone#3	$(-50000, 130000, 12000)$
Velocity of drone#3	$(60.0, 40.0, 0)$
Initial position of drone#4	$(50000, 111000, 12000)$
Velocity of drone#4	$(50.0, 35.0, 0)$
LNA magnification	160 dB
Center frequency of the receiver f_r	315.425 MHz

where g_x and g_y are the true horizontal and vertical coordinates of the target, while $\hat{g}_{x,k}$and $\hat{g}_{y,k}$ are the corresponding estimates given by the particle filtering algorithm.

5.3 The Experiment Results

In this experiment, we use $N_p = 1000$ particles. In the initialization step, we randomly generate particles, and each particle represents a guess of the position of the target. The particle initialization result is shown in Fig. 2. It can be seen that the particles are evenly distributed within the state space in which the target may exist.

As more data are assimilated, it is expected that the particles will converge to the true position of the target. We show the data assimilation results at $t = 6$ in Figs. 3a and 3b. We can see that in the sampling step (Fig. 3a), the particles that are close to the target are assigned larger weights (see the different colors); After resampling (Fig. 3b), the particles with larger weights are kept for the data assimilation at the next time step, and consequently the probability distribution

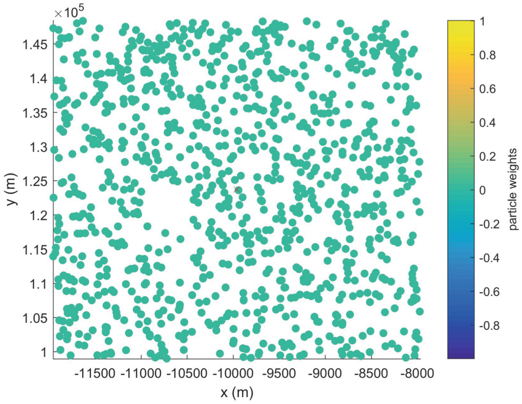

Fig. 2. The particle initialization result (the true target position is represented by a black cross)

of the estimated target position will gradually converge to the true distribution of the target (see that the area of the particle dispersion gradually shrinks).

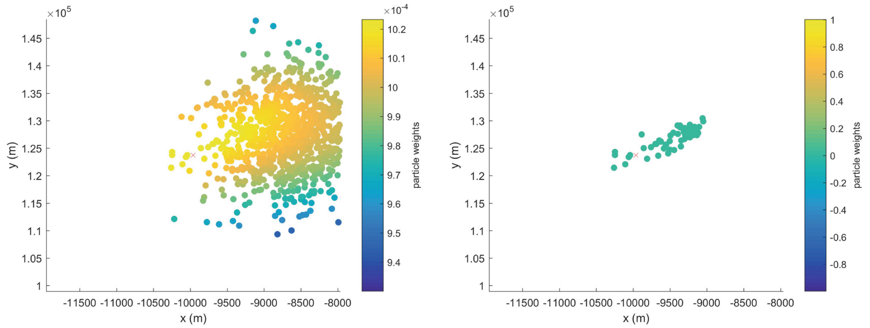

(a) The sampling results (b) The resampling results

Fig. 3. The data assimilation results at $t = 6$ (the true target position is represented by a red cross) (Color figure online)

The estimated position of the target at different time steps is shown in Figs. 4a and 4b. Based on the estimated positions at different steps, we also calculate the performance indicators defined in Eq. (9), and the values are:

$$RMSE_x = 987.7626\ m$$
$$RMSE_y = 6476\ m$$

and the relative errors are $RMSE_x/g_x \times 100\% = 9.92\%, RMSE_y/g_y \times 100\% = 5.24\%$. These results show that the proposed approach can accurately locate the target.

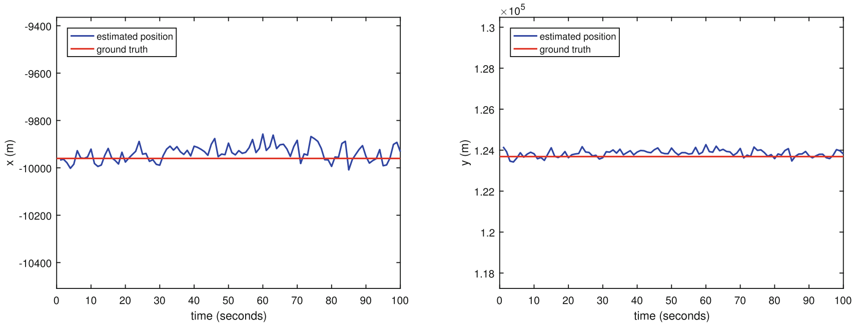

(a) The x-coordinate (b) The y-coordinate

Fig. 4. The estimated position of the target

6 Conclusions and Future Work

Locating enemy targets via their electromagnetic radiation signal is vital to block and attack the enemy targets at an earlier stage. In this paper, we propose a novel electromagnetic radiation source localization method based on dynamic data driven simulations (DDDS). Firstly, we model the spatial propagation process of the electromagnetic radiation signal emitted from the target, and then we assume a proper model for the noisy measurements. Based on these two models, we design a particle filter based localization method to locate the target. We adopt the identical-twin experiment to test and validate the proposed approach, and the experiment results show that the relative localization errors are within 10% of the true target positions, which prove that the propose approach can accurately locate the target using noisy electromagnetic radiation signals, and is also robust to errors both in the model and in the data.

Future work is planned in the following directions. First, we need to test the effectiveness of the approach when the target is moving, since this experiment assumes that the target keeps still. Second, more realistic electromagnetic radiation process models will be researched.

Acknowledgments. This research is supported by the National Natural Science Fund of China (Grant No. 62103428) and the Natural Science Fund of Hunan Province (Grant No. 2021JJ40702).

References

1. Liu, W.: Radio direction-finding and location research in the radio monitoring. Master's thesis, Xihua University (2013)
2. Li, Z., Braun, T., Zhao, X., Zhao, Z., Fengye, H., Liang, H.: A narrow-band indoor positioning system by fusing time and received signal strength via ensemble learning. IEEE Access **6**, 9936–9950 (2018)

3. Wang, Y., Ho, K.C.: Unified near-field and far-field localization for AOA and hybrid AOA-TDOA positionings. IEEE Trans. Wireless Commun. **17**(2), 1242–1254 (2018)
4. Liu, Y., Guo, F., Yang, L., Jiang, W.: An improved algebraic solution for TDOA localization with sensor position errors. IEEE Commun. Lett. **19**(12), 2218–2221 (2015)
5. Xiaolin, H.: Dynamic data driven simulation. SCS M&S Mag. **II**(1), 16–22 (2011)
6. Xie, X.: Data assimilation in discrete event simulations. Ph.D. thesis, Delft University of Technology (2018)
7. Nichols, N.: Data assimilation: aims and basic concepts. In: Swinbank, R., Shutyaev, V., Lahoz, W.A. (eds.) Data Assimilation for the Earth System, pp. 9–20. Springer, Dordrecht (2003). https://doi.org/10.1007/978-94-010-0029-1_2
8. Arulampalam, S., Maskell, S., Gordon, N., Clapp, T.: A tutorial on particle filters for online nonlinear/non-Gaussian Bayesian tracking. IEEE Trans. Signal Process. **50**(2), 174–188 (2002)
9. Djurić, P., Kotecha, J., Zhang, J., Huang, Y., Ghirmai, T., Bugallo, M., Miguez, J.: Particle filtering. IEEE Signal Process. Mag. **20**(5), 19–38 (2003)
10. Zeigler, B., Praehofer, H., Kim, T.G.: Theory of Modeling and Simulation: Integrating Discrete Event and Continuous Complex Dynamic Systems, 2nd edn. Academic Press, Cambridge (2000)
11. Lahoz, W.A., Khattatov, B., Menard, R.: Data Assimilation: Making Sense of Observations, 1st edn. Springer, Heidelberg (2010). https://doi.org/10.1007/978-3-540-74703-1
12. Darema, F.: Dynamic data driven applications systems: a new paradigm for application simulations and measurements. In: Bubak, M., van Albada, G.D., Sloot, P.M.A., Dongarra, J. (eds.) ICCS 2004. LNCS, vol. 3038, pp. 662–669. Springer, Heidelberg (2004). https://doi.org/10.1007/978-3-540-24688-6_86
13. Darema, F.: Dynamic data driven applications systems: new capabilities for application simulations and measurements. In: Sunderam, V.S., van Albada, G.D., Sloot, P.M.A., Dongarra, J.J. (eds.) ICCS 2005. LNCS, vol. 3515, pp. 610–615. Springer, Heidelberg (2005). https://doi.org/10.1007/11428848_79
14. Bouttier, F., Courtier, P.: Data assimilation concepts and methods. Meteorological Training Course Lecture Series, ECMWF (European Centre for Medium-Range Weather Forecasts) (1999)
15. Gu, F.: Dynamic data driven application system for wildfire spread simulation. Ph.D. thesis, Georgia State University (2010)
16. Bai, F., Guo, S., Hu, X.: Towards parameter estimation in wildfire spread simulation based on sequential Monte Carlo methods. In: Proceedings of the 44th Annual Simulation Symposium, Boston, MA, USA, pp. 159–166 (2011)
17. Xue, H., Gu, F., Hu, X.: Data assimilation using sequential Monte Carlo methods in wildfire spread simulation. ACM Trans. Model. Comput. Simul. **22**(4), 23:1–23:25 (2012)